General Disclaimer

One or more of the Following Statements may affect this Document

- This document has been reproduced from the best copy furnished by the organizational source. It is being released in the interest of making available as much information as possible.

- This document may contain data, which exceeds the sheet parameters. It was furnished in this condition by the organizational source and is the best copy available.

- This document may contain tone-on-tone or color graphs, charts and/or pictures, which have been reproduced in black and white.

- This document is paginated as submitted by the original source.

- Portions of this document are not fully legible due to the historical nature of some of the material. However, it is the best reproduction available from the original submission.

X-552-69-256
PREPRINT

NASA TM X- 63695

ANALYTIC DETERMINATION OF CAMERA OPERABILITY STATUS CONSIDERING DYNAMIC SOLAR CONFLICT FOR THE RADIO ASTRONOMY EXPLORER SATELLITE

HARVEY WALDEN

MAY 1969

GSFC —— **GODDARD SPACE FLIGHT CENTER** ——
GREENBELT, MARYLAND

ANALYTIC DETERMINATION OF CAMERA OPERABILITY STATUS

CONSIDERING DYNAMIC SOLAR CONFLICT

FOR THE RADIO ASTRONOMY EXPLORER SATELLITE

Harvey Walden

May 1969

GODDARD SPACE FLIGHT CENTER
Greenbelt, Maryland

ABSTRACT

An analytic method is formulated which is capable of predicting times unsuitable for useful vidicon camera operation for the Radio Astronomy Explorer satellite due to solar inclusion within the cameras' conical fields of view. The vidicon cameras, mounted within the central hub of the gravity-gradient-stabilized spacecraft, measure the 750-foot cruciform antenna boom tip positions, providing information of importance in determining the flexible Vee-antenna patterns so as to enable reduction of experimental radio astronomy data as well as for dynamics studies. A computational algorithm is developed which calculates, for each time point, the angle between the sun line referenced to the spacecraft hub center and the camera field of view axis, for each of the two vidicons positioned to observe the deformations of the upper (i.e., directed toward the galactic sphere) booms. These calculations require knowledge of certain spacecraft configuration parameters as well as ephemerides of the sun center position and spacecraft hub center position and velocity components. The analysis leading to the determination of the camera operability status predictions takes into account the effects of the skewed libration damper rod causing a static yaw bias of the satellite hub attitude, but it does not consider possible dynamic attitude librations resulting from coupling with the antenna boom flexural deformations. Numerical results from the adaption of the computational algorithm as a digital computer program are presented in tabular and graphical form. The sun line-camera axis angles display regular oscillatory variations with approximately the same period as that of the orbital anomalistic period of the satellite. The oscillatory variations are continuously perturbed by the slowly-varying shift in the orientation of the sun line relative to the satellite orbital plane so that, over the course of many orbital periods, the camera operability constant-status time intervals change markedly.

CONTENTS

ANALYTIC DETERMINATION OF CAMERA OPERABILITY STATUS
CONSIDERING DYNAMIC SOLAR CONFLICT
FOR THE RADIO ASTRONOMY EXPLORER SATELLITE

by
Harvey Walden
Goddard Space Flight Center

STATEMENT OF THE PROBLEM

Measurements of antenna boom tip positions for the Radio Astronomy Explorer (RAE-A) satellite are obtained from photographs taken by cameras mounted within the rigid central core (the "hub") of the spacecraft. Because of their great length and flexibility, various disturbing forces such as solar pressure, thermal bending, and spacecraft hub libration tend to bend the 750-foot antenna booms from their unperturbed positions. The boom tip positions as a function of time are of interest in determining the shape and pointing direction of the Vee-antenna patterns so as to enable reduction of the experimental radio astronomy data received by the directive antennae. The magnitude, direction, and frequency of the boom tip deflections about the unperturbed positions are also important for dynamics studies. In order to take useable photographs of the boom tip positions, commands from Earth-based tracking stations to operate the camera shutters must be transmitted at times corresponding to those intervals when the appropriate camera's field of view does not contain the sun. The cameras are protected by a sun sensing device which inhibits opening of the shutters when the sun is contained within the camera field of view. This feature prevents the camera from suffering a solar burn and possible permanent damage to the optical sensitivity of the system. It is the purpose of this paper to determine the analytical dynamic conditions necessary for inclusion of the sun within a camera field of view so that predictions of times unsuitable for useful camera operation may be made.

SPACECRAFT CONFIGURATION

The scientific objective of the RAE-A satellite (Reference 1) is to investigate and measure low-frequency radio emissions from solar, galactic, and extragalactic sources as a function of intensity, frequency, source direction, and time. The satellite is meant to provide, at frequencies normally below those intercepted by the Earth's ionosphere, the first radio-signal map of our galaxy.

1

The RAE-A satellite (also designated Explorer 38), managed by the NASA Goddard Space Flight Center, was launched from the Western Test Range on July 4, 1968 and is expected to have a minimum operational lifetime of one year. The satellite has assumed a near-circular (eccentricity of approximately 0.001) orbit at a 59-degree inclination, retrograde, with an altitude of approximately 5850 kilometers and an anomalistic period of 224 minutes. The non-spinning spacecraft is passively stabilized by the gravity-gradient method of three-axes control.

The RAE-A satellite consists of a rigid hub in the shape of a cylinder with truncated conical sections at each end, a rigid single-degree-of-freedom skewed libration damper (Reference 2), and four identical 750-foot flexible booms of one-half-inch-diameter hollow tubular cross section. The Vee-antennae are arranged in a cruciform configuration, i.e., forming a large "X" with the spacecraft hub at the center, with one Vee-antenna directed toward the Earth and the other toward the galactic sphere. The antenna booms forming each Vee-configuration are nominally spaced 60 degrees apart. The rigid single-degree-of-freedom damper rod is effectively hinged at the spacecraft hub and spring restrained to provide inertial coupling that permits the attitude motions about all three axes to be damped. Damper booms extend from each side of the libration damper mechanism housed in the spacecraft hub at an angle of approximately 65 degrees from the plane of the double-Vee antenna. These booms extend 315 feet from the center of the spacecraft.

The mechanism for observing the antenna boom positions consists (Reference 3) of a slow-scan television system formed of two camera-head assemblies, one for the upper (i.e., directed toward the galactic sphere) and another for the lower booms. Each camera assembly contains, in one integrated camera housing, two half-inch electromagnetic vidicons, each equipped with a lens, a sun sensor, and a shutter. Each vidicon-lens combination can view the angular positions of small sun-illuminated targets located at the tips of the 750-foot antenna booms. Each of the four vidicons has a 60-degree field of view whose conical axis coincides (Reference 4) with the unperturbed position of its corresponding antenna boom. The camera housing is designed to maintain this preset pointing angle to within ±0.1 degree as referenced to the mounting surface. The television system is able to measure the angular positions of the boom tips to within 0.5 degrees.

It is possible to select which of the upper and lower camera assemblies is to be activated, but the camera electronics provide automatic sequencing between the two vidicons within a camera assembly once operation is initiated. The camera shutters open if the sun is not in the field of view of the sun sensor provided as a protective feature for each vidicon-lens assembly. The field of view of the sun sensor is slightly larger than the nominal 60-degree circular field of the vidicon in order to protect against possible reflections of the sun off the solar paddles or other portions of the spacecraft configuration. If the sun does enter the sensor field of view, the shutter is inhibited from opening.

MATHEMATICAL MODEL

The composite RAE satellite is shown in Figure 1. It consists of a rigid hub which may be represented (Reference 5) mathematically as a "point inertia" (i.e., a mass having infinitesimal

dimensions but with well-defined principal axes and moments of inertia), a rigid single-degree-of-freedom damper rod hinged at its center of mass, and four identical flexible booms cantilevered to the hub. In Figure 1, the dashed lines represent the undeformed straight-line boom positions forming nominally $\theta = 30°$ angles with the vertical axis. The solid curved lines represent symmetric deflections of the antenna booms toward the vertical caused by the gravity gradient. In practice, there will be other, in general asymmetric, deflections in the booms caused by thermal effects, possible warpage, etc. The axes of the fields of view of the respective vidicon cameras are aligned along the dashed lines. Note the nomenclature introduced for the four booms: the "upper" booms are those pointing toward the celestial sphere and the "leading" booms are those pointing in the direction of orbital motion.
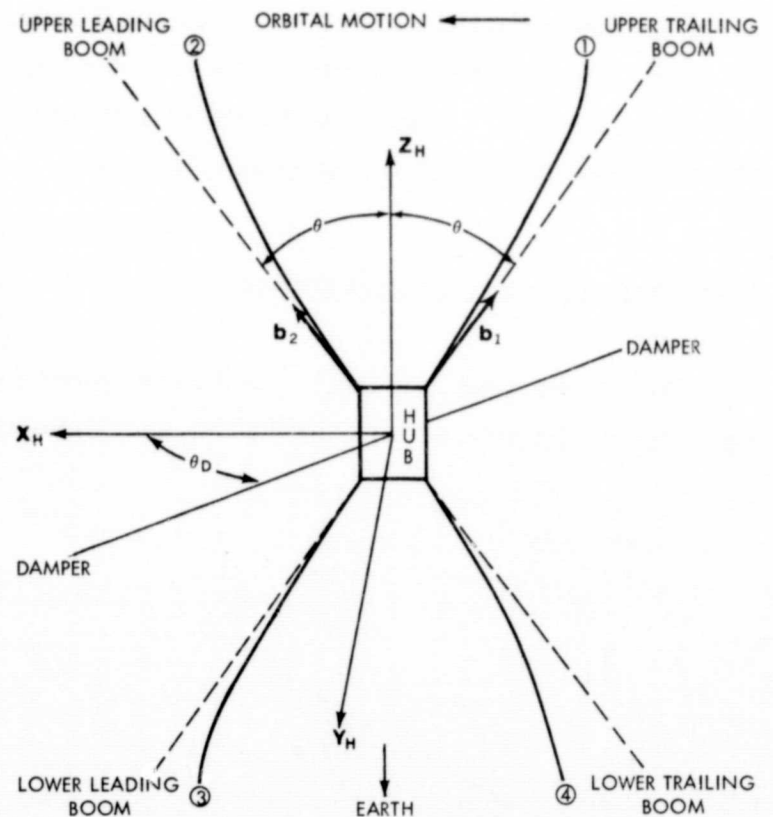

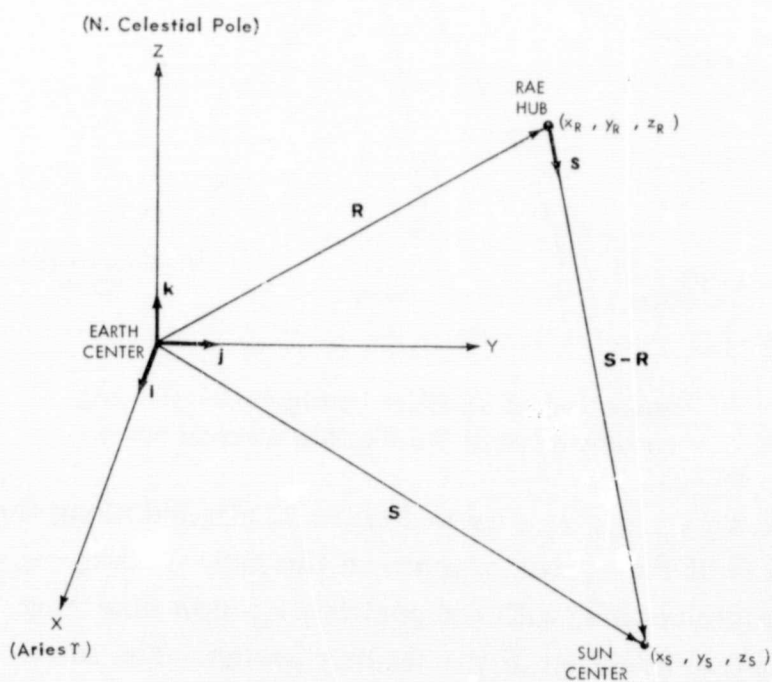Figure 1—RAE satellite configuration showing nomenclature of the flexible antenna booms.

Define an orthogonal unit set of body-fixed axes (x_H, y_H, z_H), as in Figure 1, aligned along the principal inertia axes of the hub and whose origin is at the center of mass of the hub. The $x_H - z_H$-plane coincides with the plane of the undeformed main booms, with the positive z_H-axis bisecting the upper 2θ Vee-angle and the positive x_H-axis in the direction of the leading booms. The libration damper rod is constrained to move in a plane containing the z_H-axis and is fixed relative to the hub at an angle θ_D from the $x_H - z_H$-plane. It is spring-restrained with a rest position in the $x_H - y_H$-plane. Define b_1 and b_2 to be unit vectors aligned along the undeformed upper trailing antenna boom and the undeformed upper leading antenna boom, respectively, as indicated in Figure 1.

An equilibrium state for the entire spacecraft configuration is defined as including the strain arising from the gradient of the Earth's gravitational field and the orbital motion of the satellite. With all booms in their strained equilibrium state and the damper at its reference position, the principal inertia axes of the composite satellite will be denoted by a unit orthogonal triad, (v_1, v_2, v_3), representing the roll, pitch, and yaw axes, respectively. It is well known that a satellite having unequal principal moments of inertia has gravity-gradient torques acting on it which tend to align the axis of least moment of inertia with the geocentric radius vector (i.e., the "local vertical"). Gyroscopic torques caused by orbital motion determine an orientation about the local vertical such that the principal axis of the greatest moment of inertia is aligned with the normal to the orbital plane. Thus, the intermediate principal axis is aligned with the velocity vector for an unperturbed circular orbit. For the RAE satellite, in a virtually circular orbit under passive three-axes gravity-gradient stabilization, the equilibrium state represents an alignment of the v_1, v_2, and v_3

principal axes along the velocity vector, the orbit normal, and the local vertical, respectively. The in-plane deformations of the main antenna booms would be as shown in Figure 1; however, it will be seen that equilibrium conditions also include deflections out of the plane of orbital motion. These out-of-plane deflections would tend to bend both leading booms toward the orbit normal and both trailing booms away from the orbit normal.

DYNAMICAL CONSIDERATIONS

Define an inertial Earth-fixed orthogonal system of coordinates, (X, Y, Z), whose origin is at the center of mass of the Earth; the X-Y plane is the equatorial plane, X points toward the vernal equinox (Υ) of date and Z is the north polar axis of rotation of date. Let the unit vector triad corresponding to this system be (i, j, k). It is assumed that the position $R(x_R, y_R, z_R)$ and velocity $V(\dot{x}_R, \dot{y}_R, \dot{z}_R)$ of the hub center of mass of the RAE satellite are known at time t, where the "dots" denote time derivatives. Also assume that the position of the center of mass of the sun $S(x_s, y_s, z_s)$ is also known at time t, with all coordinates given in the above inertial system. As indicated in Figure 2, a unit vector from the hub center in the direction of the sun center is given by

$$s \equiv \frac{S - R}{|S - R|} = is_1 + js_2 + ks_3 . \qquad (1)$$

Figure 2—Inertial Earth-fixed coordinate system with positions of RAE spacecraft hub center and sun center indicated.

The components of s are

$$s_1 = (x_s - x_R)/\triangle ,$$

$$s_2 = (y_s - y_R)/\triangle ,$$

and

$$s_3 = (z_s - z_R)/\triangle , \qquad (2)$$

where

$$\triangle = |S - R| = \sqrt{(x_s - x_R)^2 + (y_s - y_R)^2 + (z_s - z_R)^2} > 0 . \qquad (3)$$

4

With the definitions of b_1 and b_2 given earlier, it is of interest to determine the angles α_1 and α_2, where

$$b_1 \cdot s = \cos \alpha_1$$

and

$$b_2 \cdot s = \cos \alpha_2 . \tag{4}$$

The three vectors involved in Equations 4 are all of unit magnitude, so α_1 and α_2 are the angles between the sun line with respect to the hub center and the axes of the fields of view for the upper trailing and the upper leading cameras, respectively. The criteria for the sun to be positioned exterior to the fields of view of cameras ① and ② are, respectively, that

$$\alpha_1 > 30°$$

and

$$\alpha_2 > 30° . \tag{5}$$

If the arccosine function is restricted to the principal range of $[-180°, 180°]$, then the Inequalities 5 are equivalent to

$$30° < \left| \arccos \left(b_1 \cdot s \right) \right| \leq 180°$$

and

$$30° < \left| \arccos \left(b_2 \cdot s \right) \right| \leq 180° . \tag{6}$$

The absolute value signs are required to eliminate the double-valued property of the arccosine function, in the sense that if $b \cdot s = \cos \alpha$, then $\arccos (b \cdot s) = \pm \alpha$, where $-180° < \pm \alpha \leq 180°$.

The problem of determining the angles α_1 and α_2 then reduces to finding the components of b_1 and b_2 in the inertial frame of reference. To do so, introduce the variables δ and γ (as in Reference 2) as measures of the angular orientation of the damper rod and a principal axis of the satellite hub (namely, x_H) to the orbital plane, respectively. Equivalently, γ measures the angle between the x_H-axis and the principal axis of the composite satellite aligned along the direction of satellite motion (namely, v_1). Refer to Figure 3. Of course, the angles δ and γ must satisfy the
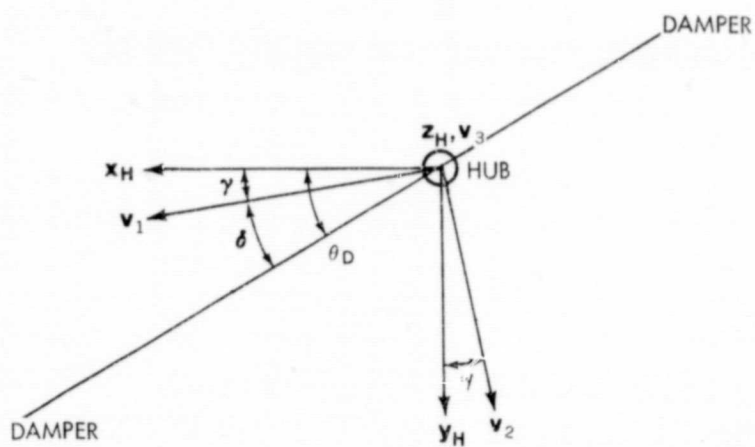
5

Figure 3—Angular relationship between the principal inertia axes of the satellite hub (x_H, y_H, z_H) and the principal inertia axes of the composite satellite (v_1, v_2, v_3).

constraint on the damper rod motion relative to the hub, which is simply

$$\theta_D = \delta + \gamma . \tag{7}$$

In effect, the fact that the damper rod is skewed relative to the principal inertia axes of the spacecraft hub causes a static yaw bias of the hub attitude about the local vertical axis v_3 of magnitude γ. It is readily seen that the relations between the hub-fixed principal axes and the composite satellite principal axes are given by

$$x_H = v_1 \cos\gamma - v_2 \sin\gamma ,$$

$$y_H = v_1 \sin\gamma + v_2 \cos\gamma ,$$

and

$$z_H = v_3 . \tag{8}$$

Since b_1 and b_2 lie in the x_H - z_H plane, their decomposition is simply

$$b_1 = - x_H \sin\theta + z_H \cos\theta$$

and

$$b_2 = + x_H \sin\theta + z_H \cos\theta , \tag{9}$$

where θ is the semi-Vee angle of the main antenna booms. Substituting from Equations 8 into Equations 9 yields

$$b_1 = - v_1 \sin\theta \cos\gamma + v_2 \sin\theta \sin\gamma + v_3 \cos\theta$$

and

$$b_2 = + v_1 \sin\theta \cos\gamma - v_2 \sin\theta \sin\gamma + v_3 \cos\theta . \tag{10}$$

6

Now (v_1, v_2, v_3) must be determined in terms of R and V at time t. Since v_3 is a unit vector in the direction of the local vertical,

$$v_3 = \frac{R}{|R|} = i\,\frac{x_R}{R} + j\,\frac{y_R}{R} + k\,\frac{z_R}{R} ,$$

(11)

where

$$R = |R| = \sqrt{x_R^2 + y_R^2 + z_R^2} > 0 .$$

(12)

Now v_2 is the unit orbit normal, so that

$$v_2 = \frac{R \times V}{|R \times V|} = \frac{1}{|R \times V|} \cdot \begin{vmatrix} i & j & k \\ x_R & y_R & z_R \\ \dot{x}_R & \dot{y}_R & \dot{z}_R \end{vmatrix} ,$$

(13)

writing the vector cross product in its usual determinant form. Expanding Equation 13,

$$v_2 = \frac{1}{|R \times V|} \left[i\left(y_R \dot{z}_R - z_R \dot{y}_R\right) + j\left(z_R \dot{x}_R - x_R \dot{z}_R\right) + k\left(x_R \dot{y}_R - y_R \dot{x}_R\right) \right]$$

(14)

or

$$v_2 = i\,\frac{N_1}{N} + j\,\frac{N_2}{N} + k\,\frac{N_3}{N} ,$$

(15)

where

$$N_1 = y_R \dot{z}_R - z_R \dot{y}_R ,$$

$$N_2 = z_R \dot{x}_R - x_R \dot{z}_R ,$$

$$N_3 = x_R \dot{y}_R - y_R \dot{x}_R ,$$

(16)

and

$$N = \sqrt{N_1^2 + N_2^2 + N_3^2} > 0 .$$

(17)

Finally, for the third member of the unit triad,

$$v_1 = v_2 \times v_3 = \begin{vmatrix} i & j & k \\ N_1/N & N_2/N & N_3/N \\ x_R/R & y_R/R & z_R/R \end{vmatrix} \tag{18}$$

or

$$v_1 = i\left(\frac{N_2 z_R - N_3 y_R}{NR}\right) + j\left(\frac{N_3 x_R - N_1 z_R}{NR}\right) + k\left(\frac{N_1 y_R - N_2 x_R}{NR}\right). \tag{19}$$

For nearly circular orbits (such as that of the RAE-A satellite), v_1 is approximately equal to the unit velocity vector, i.e.,

$$v_1 \cong \frac{V}{|V|} = i\frac{\dot{x}_R}{V} + j\frac{\dot{y}_R}{V} + k\frac{\dot{z}_R}{V}, \tag{20}$$

where

$$V = \sqrt{\dot{x}_R^2 + \dot{y}_R^2 + \dot{z}_R^2} > 0. \tag{21}$$

Now b_1 and b_2 can be written in terms of components in the inertial Earth-fixed frame of coordinates by substitution of Equations 11, 15, and 19 into Equations 10, as follows:

$$b_1 = i\left[-\sin\theta\cos\gamma\left(\frac{N_2 z_R - N_3 y_R}{NR}\right) + \sin\theta\sin\gamma\left(\frac{N_1}{N}\right) + \cos\theta\left(\frac{x_R}{R}\right)\right]$$

$$+ j\left[-\sin\theta\cos\gamma\left(\frac{N_3 x_R - N_1 z_R}{NR}\right) + \sin\theta\sin\gamma\left(\frac{N_2}{N}\right) + \cos\theta\left(\frac{y_R}{R}\right)\right]$$

$$+ k\left[-\sin\theta\cos\gamma\left(\frac{N_1 y_R - N_2 x_R}{NR}\right) + \sin\theta\sin\gamma\left(\frac{N_3}{N}\right) + \cos\theta\left(\frac{z_R}{R}\right)\right]$$

and

$$b_2 = i\left[+\sin\theta\cos\gamma\left(\frac{N_2 z_R - N_3 y_R}{NR}\right) - \sin\theta\sin\gamma\left(\frac{N_1}{N}\right) + \cos\theta\left(\frac{x_R}{R}\right)\right]$$

$$+ j\left[+\sin\theta\cos\gamma\left(\frac{N_3 x_R - N_1 z_R}{NR}\right) - \sin\theta\sin\gamma\left(\frac{N_2}{N}\right) + \cos\theta\left(\frac{y_R}{R}\right)\right]$$

$$+ k\left[+\sin\theta\cos\gamma\left(\frac{N_1 y_R - N_2 x_R}{NR}\right) - \sin\theta\sin\gamma\left(\frac{N_3}{N}\right) + \cos\theta\left(\frac{z_R}{R}\right)\right] \tag{22}$$

If B_i and C_i are defined as

$$B_1 \equiv \frac{\sin\theta\cos\gamma}{NR} ,$$

$$B_2 \equiv \frac{\sin\theta\sin\gamma}{N} ,$$

$$B_3 \equiv \frac{\cos\theta}{R} , \tag{23}$$

and

$$C_1 \equiv N_2 z_R - N_3 y_R ,$$

$$C_2 \equiv N_3 x_R - N_1 z_R ,$$

$$C_3 \equiv N_1 y_R - N_2 x_R , \tag{24}$$

then the following simpler form for Equations 22 results:

$$
\begin{aligned}
b_1 = \; & i\left(-B_1 C_1 + B_2 N_1 + B_3 x_R\right) \\
& + j\left(-B_1 C_2 + B_2 N_2 + B_3 y_R\right) \\
& + k\left(-B_1 C_3 + B_2 N_3 + B_3 z_R\right)
\end{aligned}
$$

and

$$
\begin{aligned}
b_2 = \; & i\left(+B_1 C_1 - B_2 N_1 + B_3 x_R\right) \\
& + j\left(+B_1 C_2 - B_2 N_2 + B_3 y_R\right) \\
& + k\left(+B_1 C_3 - B_2 N_3 + B_3 z_R\right) .
\end{aligned}
\tag{25}
$$

The scalar dot products $b_1 \cdot s$ and $b_2 \cdot s$ are now readily evaluated as

$$b_1 \cdot s = b_{1x} s_1 + b_{1y} s_2 + b_{1z} s_3 = \cos\alpha_1$$

and

$$b_2 \cdot s = b_{2x} s_1 + b_{2y} s_2 + b_{2z} s_3 = \cos\alpha_2 , \tag{26}$$

9

where

$$b_{1x} \equiv -B_1 C_1 + B_2 N_1 + B_3 x_R ,$$

$$b_{1y} \equiv -B_1 C_2 + B_2 N_2 + B_3 y_R ,$$

$$b_{1z} \equiv -B_1 C_3 + B_2 N_3 + B_3 z_R , \qquad (27)$$

and

$$b_{2x} \equiv B_1 C_1 - B_2 N_1 + B_3 x_R ,$$

$$b_{2y} \equiv B_1 C_2 - B_2 N_2 + B_3 y_R ,$$

$$b_{2z} \equiv B_1 C_3 - B_2 N_3 + B_3 z_R . \qquad (28)$$

Finally, the criteria for the sun to be positioned exterior to the fields of view of the upper trailing and the upper leading cameras are given in Equations 6 above.

REMARKS ON THE METHOD PRESENTED

Of the three vectors involved in the final result for $\cos \alpha_1$ and $\cos \alpha_2$ in Equations 26, note that the components of s depend upon the coordinates of the sun (x_s, y_s, z_s) and of the satellite hub center (x_R, y_R, z_R) in the inertial Earth-fixed frame, while the components of b_1 and b_2 depend on the coordinates (x_R, y_R, z_R) and velocities $(\dot{x}_R, \dot{y}_R, \dot{z}_R)$ of the hub center in the inertial frame plus trigonometric functions of spacecraft parameters θ and γ. Values for the semi-Vee angle θ of the main antenna booms and for the equilibrium yaw bias γ (equivalently, the angle of separation between the principal axes of the composite spacecraft and the hub principal axes) will be discussed at greater length below.

It ought to be noted that the method of analysis presented above does not consider possible dynamic attitude librations caused by coupling with the antenna boom flexural deformations. Other simplifying assumptions made in this analysis include the idealization of the solar disc to a point source and of the rigid central hub of the spacecraft to a point inertia. The effects of these assumptions upon the final results are deemed to be fairly negligible. There is, further, the possibility of chance solar reflections off some portion of the spacecraft configuration entering one of the camera's field of view, an occurrence which cannot readily be predicted. However, the chances of such a random solar reflection are minimized as the angles α_1 and α_2 between the sun line referenced to the satellite hub center and the camera field of view axes approach 180 degrees. Attainment of this maximum 180-degree angular separation is equivalent to a condition of anti-parallelism between the sun line and camera axis.

10

COMPUTATIONAL ALGORITHM

Given the semi-Vee angle θ of the main antenna booms and the equilibrium yaw bias angle γ, the sun center position (x_s, y_s, z_s) at time t, and the spacecraft hub center position (x_R, y_R, z_R) and velocity $(\dot{x}_R, \dot{y}_R, \dot{z}_R)$, also at time t, the determination of the criteria for the sun to be positioned exterior to the fields of view of the upper cameras proceeds as follows. Calculate:

1. $\triangle$ by Equation 3.

2. s_1, s_2, s_3 by Equations 2.

3. N_1, N_2, N_3 by Equations 16.

4. N by Equation 17.

5. R by Equation 12.

6. B_1, B_2, B_3 by Equations 23.

7. C_1, C_2, C_3 by Equations 24.

8. b_{1x}, b_{1y}, b_{1z} by Equations 27.

9. b_{2x}, b_{2y}, b_{2z} by Equations 28.

10. $\cos\alpha_1$, $\cos\alpha_2$ by Equations 26.

Then the required criteria are provided by the Inequalities 5 or, equivalently, by those of the Inequalities 6.

NUMERICAL RESULTS

For the Radio Astronomy Explorer satellite, the semi-Vee angle θ of the main antenna booms is nominally 30 degrees. According to the best available numerical data (Reference 6), the value for the semi-Vee angle of the upper leading main boom is 28 degrees and of the upper trailing boom is 27.5 degrees. The equilibrium yaw bias angle γ is calculated (Reference 5) on the basis of standard spacecraft parameters to be 0.127 radians or 7.3 degrees. However, processing of the attitude sensor data returned from the spacecraft (Reference 7) seems to indicate a mean value for the yaw hub attitude angle of approximately 14 degrees. The reason for this discrepancy between calculated and observed values for γ is not fully known and is currently under investigation.

The computational algorithm provided above has been adapted in the form of a digital computer program which predicts time intervals unsuitable for useful camera operation for the RAE-A satellite. Two sets of ephemerides are provided to this computer program as input; one ephemeris contains the position of the sun in inertial Earth-fixed coordinates at regular time points throughout a specified time period, and the other ephemeris contains the position and velocity components

of the spacecraft in inertial Earth-fixed coordinates for the same set of time points. In actual practice, the time points are generally given at one-minute intervals for a period spanning approximately one week. In the numerical applications to be described, values of the spacecraft parameters chosen were θ = 28.0 degrees and γ = 14.0 degrees. The computer program, on the basis of this input data, then calculates, for each time point in the period, the angles α_1 and α_2 between the sun line and the camera field of view axis for each of the two upper boom vidicons.

Figures 4 and 5 illustrate the variation of the angles α_1 and α_2, respectively, over a period of time of 8 hours and 20 minutes, with the camera operability criterion indicated at an angle of 30 degrees. From Figure 4, it can be seen that the sun line-camera axis angle α_1 for the upper trailing vidicon varies between 21 degrees and 172 degrees for an amplitude width of 151 degrees. The period between successive minima or successive maxima is found to be 3 hours and 51 minutes. Figure 5 indicates that the angle α_2 for the upper leading camera varies between 8 degrees and 159 degrees. Its amplitude width is also 151 degrees but has been depressed by an amount equal to 13 degrees relative to the variation of α_1. The period between successive like extrema is again found to be 3 hours and 51 minutes. Investigation of the phase difference between α_1 and α_2 leads to the result that the variation of α_2 precedes that of α_1 by a phase shift of 35 minutes. Table 1 lists the camera operability conditions for a 24-hour period, the first 8 hours and 20 minutes of which (i.e., from 00:00 to 08:20) correspond to the time period covered by Figures 4 and 5. For each time interval in the left column, the status of the upper cameras is given in the center column, and the duration of each "constant-status" time interval is displayed in the right column. In point of fact, Table 1 corresponds to actual camera operability condition predictions generated for April 14, 1969 (Universal Times).

Figures 6 and 7 illustrate the variation of α_1 and α_2, respectively, over a different time period of 8 hours and 20 minutes. Table 2 lists the camera operability conditions for a 24-hour period,
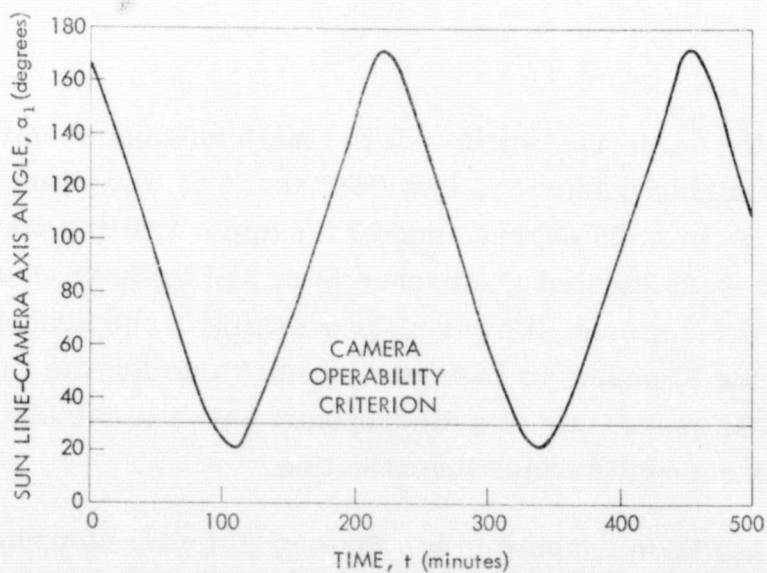

Figure 4—Variation in the angle between the sun line (referenced to the spacecraft hub center) and the camera field of view axis, for the upper trailing boom camera on Date 1.
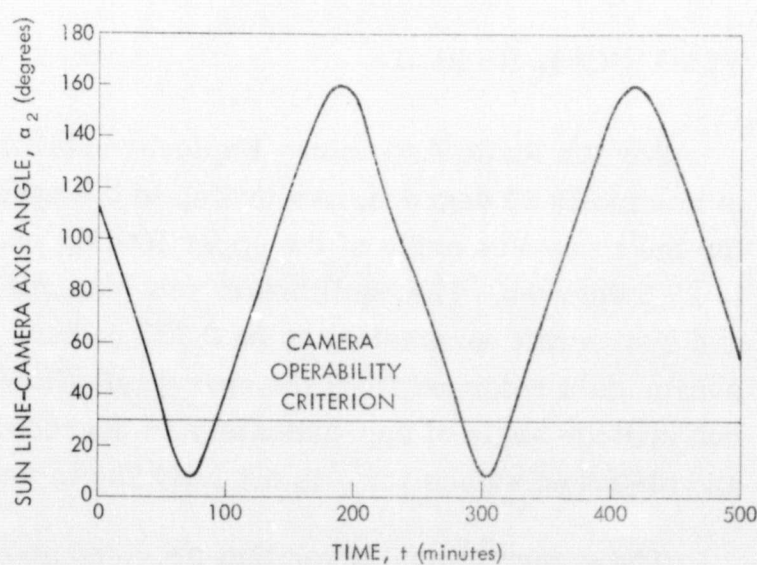
Figure 5—Variation in the angle between the sun line (referenced to the spacecraft hub center) and the camera field of view axis, for the upper leading boom camera on Date 1.

12

Table 1
Camera Operability Conditions (Date 1)

Time Interval (Hours: Minutes)	Camera Status*	Duration of Interval (Hours: Minutes)
00:00 — 00:54	Both	≥ 00:54
00:55 — 01:32	Trailing	00:37
01:33 — 01:34	Both	00:01
01:35 — 02:02	Leading	00:27
02:03 — 04:45	Both	02:42
04:46 — 05:23	Trailing	00:37
05:24 — 05:25	Both	00:01
05:26 — 05:52	Leading	00:26
05:53 — 08:35	Both	02:42
08:36 — 09:13	Trailing	00:37
09:14 — 09:15	Both	00:01
09:16 — 09:42	Leading	00:26
09:43 — 12:26	Both	02:43
12:27 — 13:03	Trailing	00:36
13:04 — 13:06	Both	00:02
13:07 — 13:32	Leading	00:25
13:33 — 16:16	Both	02:43
16:17 — 16:54	Trailing	00:37
16:55 — 16:56	Both	00:01
16:57 — 17:23	Leading	00:26
17:24 — 20:06	Both	02:42
20:07 — 20:44	Trailing	00:37
20:45 — 20:46	Both	00:01
20:47 — 21:13	Leading	00:26
21:14 — 23:57	Both	02:43
23:58 — 24:00	Trailing	≥ 00:02

*The designations "leading," "trailing," and "both" indicate that the spacecraft's upper leading camera only, upper trailing camera only, or both upper cameras, respectively, are operable within the time interval specified. The operability criterion is defined to be a sun line-camera axis angle exceeding 30 degrees.
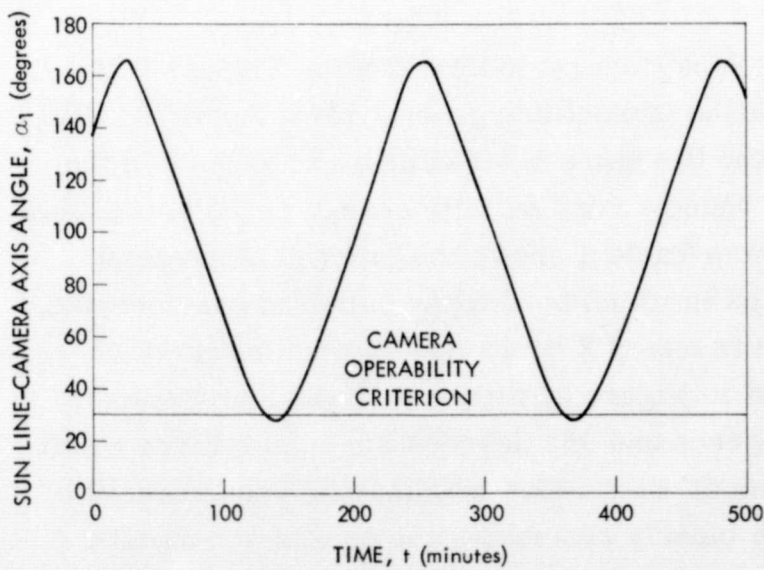

Figure 6—Variation in the angle between the sun line (referenced to the spacecraft hub center) and the camera field of view axis, for the upper trailing boom camera on Date 2.
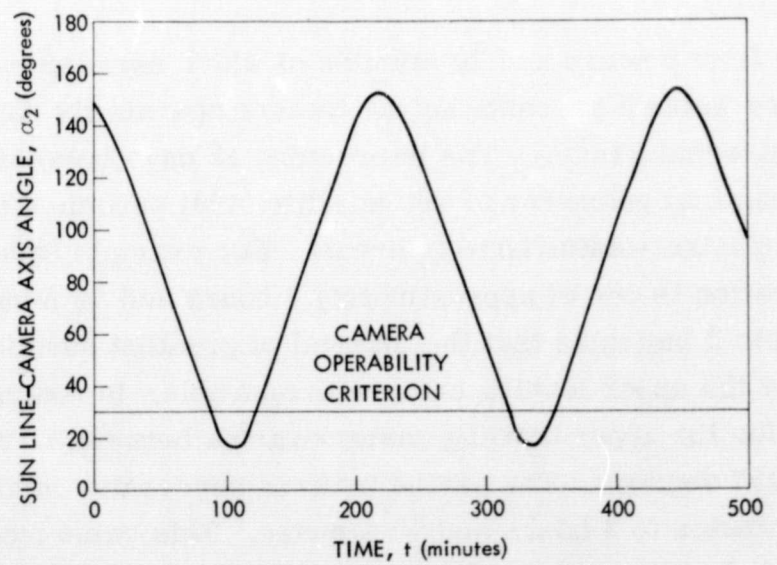

Figure 7—Variation in the angle between the sun line (referenced to the spacecraft hub center) and the camera field of view axis, for the upper leading boom camera on Date 2.

13

Table 2

Camera Operability Conditions (Date 2)

Time Interval (Hours: Minutes)	Camera Status*	Duration of Interval (Hours: Minutes)
00:00 — 01:29	Leading	≥ 01:29
01:30 — 02:03	Trailing	00:33
02:04 — 02:14	Leading	00:10
02:15 — 02:27	Both	00:12
02:28 — 05:17	Leading	02:49
05:18 — 05:52	Trailing	00:34
05:53 — 06:02	Leading	00:09
06:03 — 06:15	Both	00:12
06:16 — 09:05	Leading	02:49
09:06 — 09:40	Trailing	00:34
09:41 — 09:51	Leading	00:10
09:52 — 10:04	Both	00:12
10:05 — 12:54	Leading	02:49
12:55 — 13:28	Trailing	00:33
13:29 — 13:39	Leading	00:10
13:40 — 13:52	Both	00:12
13:53 — 16:42	Leading	02:49
16:43 — 17:16	Trailing	00:33
17:17 — 17:28	Leading	00:11
17:29 — 17:40	Both	00:11
17:41 — 20:30	Leading	02:49
20:31 — 21:05	Trailing	00:34
21:06 — 21:16	Leading	00:10
21:17 — 21:28	Both	00:11
21:29 — 24:00	Leading	≥ 02:31

*The designations "leading," "trailing," and "both" indicate that the spacecraft's upper leading camera only, upper trailing camera only, or both upper cameras, respectively, are operable within the time interval specified. The operability criterion is defined to be a sun line-camera axis angle exceeding 30 degrees.

the first 8 hours and 20 minutes of which correspond to the time period covered by Figures 6 and 7. Here Table 2 presents actual camera operability condition predictions generated for April 29, 1969 (Universal Times). The intervening 15 days between the two dates have witnessed a change in the dynamical geometry of the satellite orbit sufficient to cause a very definite change in the succession of constant-status time intervals. For example, whereas Table 1 shows the interval of greatest duration is one of approximately 2 hours and 42 minutes in which both upper cameras are operable, Table 2 indicates that the interval of greatest duration is one of 2 hours and 49 minutes in which only the upper leading camera is operable. In contrast to Figure 4, Figure 6 shows that the angle a_1 for the upper trailing camera varies between 28 degrees and 165 degrees for an amplitude width of 137 degrees. The period between successive minima or successive maxima has been reduced by 3 minutes to 3 hours and 48 minutes. This value more closely resembles the orbital anomalistic period of the satellite, which is 3 hours and 44 minutes. Also, in contrast to Figure 5, Figure 7 shows the angle a_2 for the upper leading camera varying between 15 and 152 degrees for the same amplitude width of 137 degrees. Again the variation of a_2 has been depressed, relative to a_1, by an

amount equal to 13 degrees. Also note that the oscillations of both α_1 and α_2 in Figures 6 and 7 are contained within envelopes symmetrically located 7 degrees within the respective envelopes containing the oscillations of α_1 and α_2 in Figures 4 and 5. The period between successive like extrema of α_2 in Figure 7 is 3 hours and 48 minutes, equal to the period of α_1 in Figure 6. Finally, the phase difference between α_1 and α_2 remains at 35 minutes, with α_2 preceding α_1.

In summary, the sun line-camera axis angles α_1 and α_2 display very regular oscillatory variations within each orbital period of the satellite's motion. From one orbital period to the next, these oscillatory variations are very slightly and continuously perturbed, this effect probably caused mainly by the slowly-varying shift in the orientation of the Earth-sun line relative to the orbital plane of the satellite. Over the course of several days, the oscillatory variations of α_1 and α_2 are sufficiently perturbed to cause appreciable changes in the camera operability constant-status time intervals within a given orbital period.

REFERENCES

1. Stone, Robert G., "RAE—1500-ft. Antenna Satellite," *Astronautics and Aeronautics*, Vol. 3, No. 3, March 1965, pp. 46-49.

2. Tinling, Bruce E. and Merrick, Vernon K., "Exploitation of Inertial Coupling in Passive Gravity-Gradient-Stabilized Satellites," *Journal of Spacecraft and Rockets*, Vol. 1, No. 4, July-August 1964, pp. 381-387.

3. Grant, M. M. and Libby, J. N., "Operational Considerations for the Radio Astronomy Explorer (A) Spacecraft," NASA Goddard Space Flight Center Document No. X-722-68-103, May 1968.

4. Davidson, Arthur C., RAE Project Management Office, NASA Goddard Space Flight Center, Private communication, January 24, 1969.

5. Newton, James K. and Farrell, James L., "Natural Frequencies of a Flexible Gravity-Gradient Satellite," *Journal of Spacecraft and Rockets*, Vol. 5, No. 5, May 1968, pp. 560-569.

6. Keat, J. E., "Final Report on RAE-A Performance at 450 ft. and During Boom Deployments from 450 ft. to 750 ft.," Vol. I: Discussion of Performance, Prepared by Westinghouse Electric Corporation, Aerospace Division for NASA Goddard Space Flight Center, February 17, 1969.

7. Werking, Roger D., Weekly RAE-A Attitude Reports (unpublished), Attitude Determination Office, NASA Goddard Space Flight Center.